FAST Observations of Ion Outflow Associated with Magnetic Storms

J. P. McFadden[1], Y. K. Tung[1], C. W. Carlson[1], R. J. Strangeway[2], E. Moebius[3], and L. M. Kistler[3]

Abstract

New observations from the FAST mission are used to study the relationship between the auroral ionospheric ion outflow and the injection of ring current plasma during magnetic storms. One set of observations follows the injection of the low energy tail of the ring current (<25 keV) at low latitudes (L-shell<4). These ions are found to be primarily of ionospheric origin and to evolve on the two hour time scale of the spacecraft orbit indicating a relatively brief injection. Higher latitude observations show intense auroral outflows are observed in both the cusp and near midnight during magnetic storms. Cusp outflows that are energetic enough to contribute hot plasma to the plasmasheet are likely lost out the magnetotail whereas nightside auroral outflows place ionospheric ions directly onto newly reconnected plasmasheet field lines. These observations suggest how substorms can play a role in the development of magnetic storms. Electrons accelerated during substorms produce waves that heat the ionospheric plasma producing intense conic outflows into the plasmasheet. The higher density plasmasheet ions are subsequently convected to the inner magnetosphere by the large convection electric fields during the magnetic storm. Without the large convection fields, the substorm outflows have no effect on Dst since these ions never reach the inner L-shells. Without substorm outflows, the plasmasheet density is relatively modest so that convection to the inner L-shells produces only small drops in Dst. In this model, it is through ionospheric ion outflows that substorms affect the development of magnetic storms.

[1] Space Sciences Lab., University of California, Berkeley, CA

[2] IGPP, University of California, Los Angeles, CA

[3] Space Science Center, University of NH, Durham, NH

1. INTRODUCTION

The sources of plasmasheet and ring current plasma are an important element in understanding the dynamics of the Earth's magnetosphere. Models that attempt to predict the "space weather" of the near Earth environment must be able to account for relative abundances of ionospheric and solar wind plasma in the magnetosphere. To distinguish these sources of plasma, one generally looks for O^+ as a proxy for an ionospheric source. When the composition is primarily H^+, it is assumed that the source is the solar wind even though the ionosphere can be a major source of H^+. *Hamilton et al.* [1988] found that the storm time ring current was primarily H^+ for moderate magnetic storms, but for the one great magnetic storm observed by AMPTE, the ring current was dominated by O^+ during the storm's maximum phase. These observations, made during solar minimum, were extended by *Daglis* [1997] who used CRRES data to show that the large magnetic storms during solar maximum were also dominated by O^+. This supports the hypothesis of *Hamilton et al.* [1988] that the initial fast Dst recovery during great magnetic storms can be explained in terms of the rapid loss of energetic ($\sim$100 keV) O^+ which has a shorter charge exchange lifetime. More recent observations point to a highly asymmetric ring current [*Grafe,* 1999; *Greenspan and Hamilton,* 2000] during the main phase of storms which is explained by drift-loss ring current models [*Kozyra et al.,* 1998; *Liemohn et al.,* 1999]. In these models both dayside outflows and charge exchange play roles in the evolution of the ring current.

Since one of the primary space weather perturbations is due to the ring current, it is important to identify the source and energization of ring current plasma. Injections of ions at geosynchronous altitudes were observed on early satellite missions [*Arnoldy and Chan,* 1969; *DeForest and McIlwain,* 1971] and explained in terms of a substorm injection boundary [*Mauk and McIlwain,* 1974]. The relationship between geosynchronous ion injections associated with substorm dipolarizations and storm related ring current ion injections has been a subject of debate [see *McPherron,* 1997, and references therein] including arguments that magnetic storms are the result of a succession of substorm ion injections. It has also been argued [*Kamide et al.,* 1997] that substorm injections are not fundamental to ring current formation since they are limited to the outer L-shells. To affect Dst during magnetic storms, ion injections must place significant plasma on the inner L-shells (L<4).

Ring current injections appear to originate in the plasmasheet as shown by particle tracing through model electric and magnetic fields [*Chen et al.,* 1994]. *Lennartsson and Sharp* [1982] and *Young et al.,* [1982] found that the plasmasheet (L>5) was typically dominated by H^+ except during disturbed times when O^+ could be significant. During the early phase of magnetic storms, the O^+/H^+ ratios were the highest and the mean plasma energies were elevated. These observations and simulations suggest that an enhanced outflow of ionospheric plasma into the plasmasheet precedes large magnetic storms and that this plasma subsequently convects or is injected into the inner magnetosphere by enhanced solar wind - magnetospheric coupling. This plasma, after betatron heating and perhaps additional nonadiabatic heating, eventually becomes the storm time ring current. The two primary sources of ionospheric outflow into the plasmasheet are the polar cusp and near midnight oval. In this paper we investigate ion injections into the inner magnetosphere and ion outflows from the cusp and midnight oval.

2. LOW LATITUDE OBSERVATIONS

We begin with an example of low latitude ion injection associated with the magnetic storm on September 22-23, 1999. Figure 1a shows the provisional Dst reached a minimum -164 during a three hour drop then gradually recovered over the next two days. Prior to the storm, the Wind spacecraft showed a southward turning of a rather large >20 nT interplanetary magnetic field at $\sim$20:35 UT on September 22, which continued for about 3 hours. This field should have reached Earth $\sim$20:50 UT and appears to have triggered a substorm with AE reaching $\sim$900 thirty minutes later. AE eventually exceeded 1500 several times over the course of the next two hours.

Plate 1 shows a series of three low latitude FAST passes (Orbits 12222, 12223, and 12224) through magnetic noon during this magnetic storm. For each orbit, the H^+, He^+, O^+, and total ion energy flux are plotted from top to bottom. Prior to orbit 12222, FAST detected no significant low latitude ions for several days. The series of plots show an injection of ions that peaks in the middle panel at 2:30 UT and begins to fade on the following orbit. Subsequent orbits show the ions at ILAT<50° disappear after a few orbits, however a more tenuous flux of O^+ ions at 50°<ILAT<60° remain discernible for two days. The

primary features of the plot are the rather abrupt energy-latitude injection boundary, the penetration of these ions to at least L=2, and the dominance of O^+ in the injection. Ion injections of this type are observed for all drops in Dst when FAST low latitude data are available.

The sharp upper cutoff of the ion flux between 5 and 10 keV marks the energy boundary where $\boldsymbol{E} \times \boldsymbol{B}$ and ∇B drifts oppose each other along the particle trajectories, resulting in longer drift times and often significant charge exchange losses before the ions reach the dayside. Below this energy cutoff, ions $\boldsymbol{E} \times \boldsymbol{B}$ drift eastward and above this cutoff the ions ∇B drift westward around the Earth. The increase in background counts near the end time of the plots, in particular the ESA plots, is due to penetrating radiation from the inner radiation belt.

We now examine another ion injection associated with a rather weak (Dst=-78) magnetic storm on March 10, 1999 (Figure 1b). The provisional Dst for early March shows this to be an active period after the recovery from a magnetic storm on March 1, with Dst fluctuating between -20 and -50 from March 2 to March 9. Low latitude ions are observed on most of these days, although they are generally weak and remain at L>3. Wind data show a fluctuating solar wind magnetic field (~5-10 nT) with short periods of southward B_z but no extended period with strong southward B_z. The AE index is also generally high, exceeding 500 one or more times each day during this period, indicating an average of several substorms per day. At the end of the day on March 9, B_z turns southward and remains southward until about 5 UT on March 10. B_z then turns northward for ~2.5 hours, then southward for another 4.5 hours, before turning northward again for an extended period (~7 hours). The magnitude of B was slightly higher (B~10 nT) on March 10 during the periods with extended B_z southward. These last two southward turnings are associated with two periods of enhanced AE index (1:40-4:30 and 7:30-10:00 UT) and low latitude ion injections observed by FAST.

Plate 2 shows the low latitude ion injections associated with the drop in Dst on March 10 (Figure 1b), with measurements made at 7-8 MLT. The low latitude ions on orbit 10083 are the product of two ion injections. The first ion injection was observed to peak near orbit 10081 (~5 UT). Those ions between 9:52 and 10:01 UT in Plate 2a are the remnants of this earlier injection, similar to the ions in Plate 1c. The more intense ions between 9:45 and 9:52 UT in Plate 2a were the second ion injection which developed into the more equatorward ion flux seen between 12:04 and 12:14 UT in Plate 2b. By orbit 10085 (Plate 2c) no ions at L<3 (ILAT< 55°) were observed and a gradual recovery of the plasmasphere's density was measured by FAST. (Note: The enhanced counts in the bottom panel of Plate 2c at 14:15 UT are primarily due to penetrating energetic electrons.)

The provisional Dst shows two minima on March 10 (Figure 1b), at 4-5 and 8-9 UT, which appear to be associated with the two ion injections seen in Plate 2. Since the low latitude ions were observed at a local time (~7:30 MLT) far from the injection region near midnight, an ~1 hour delay must be expected between the injection and arrival of convecting ions at FAST (~9:45 UT in Plate 2a). The estimated injection time (~8:45) is consistent with the minimum Dst value at 8-9 UT. This Dst minimum is lower than the minimum at 4-5 UT, which is consistent with two ion injections being present at 8-9 UT as seen in Plate 2a.

We hypothesize that enhanced auroral activity or substorms, as indicated by AE, are responsible for the initial ion outflow into the plasmasheet, and that subsequent convection injected these ions into the inner magnetosphere. It also appears that the first ion injection convected out of the inner magnetosphere shortly after 10 UT since Dst increased from -62 to -35 by 10-11 UT. Similar changes in Dst are observed with the drift-loss ring current model [*Kozyra et al.,* 1998; *Liemohn et al.,* 1999]. Since Dst remained in the -30 to -40 range for most of the day, one might anticipate that the second ion injection remained within the inner magnetosphere when it decoupled from the sunward flows. From the decrease in the southward component of the IMF B_z at ~10 UT, the eventual northward turning of B_z at ~11:30 UT, the drop in AE index to below 500 at ~10 UT, and drop in AE below 200 at ~11:45 UT, the decoupling likely occurred between 10 and 12 UT, with the more probable time closer to 10 UT. Since FAST detected low latitude ions at L<3 at ~12 UT (Plate 2b) and observed their subsequent disappearance on the following orbits, it appears that co-rotation shifted these ions to later local times. Weaker fluxes of ions at L<3 were observed 24 hours later as one would expect if the ions were trapped on co-rotational orbits. The abrupt disappearance of these ions in Plate 2c strongly suggests that these low latitude injections are localized in both space and time. In the following sections we will look closely at auroral ion outflows in an attempt to inves-

tigate whether auroral activity can account for these low latitude ions.

3. CUSP OUTFLOW

The polar cusp has long been known to be a source of ionospheric outflow [*Lockwood,* 1985; *Moore et al.,* 1996]. *Yau et al.* [1985] presented statistics of ion outflow which showed the largest average outflows were in the vicinity of the cusp. However statistical studies are not necessarily representative of the large outflows observed during active periods associated with magnetic storms. Instead we examine an individual magnetic storm and look for the source of ionospheric outflow in the cusp and compare timing of this outflow with the drops in Dst. We begin with a summary of the cusp outflows observed by FAST for the September 24, 1998 magnetic storm.

This magnetic storm is associated with a CME that reached the magnetopause at ~23:45 UT on September 24. Using observations from the Polar spacecraft, *Moore et al.* [1999] showed energetic ion outflows were observed in the northern cusp region for several hours after the arrival of the CME, with enhanced outflows continuing during the Polar southern auroral pass seven hours later. Plate 3 shows the FAST northern auroral crossings on the first three orbits during the September 25, 1998 magnetic storm. Orbit 8276 shows an enhanced ion outflow in the cusp region between 00:05 and 00:10 UT that exceeds $10^{10}/\mathrm{cm}^2$-s when projected to 100 km. On orbit 8277, cusp outflows are reduced by nearly an order of magnitude to $\sim 2 \times 10^9/\mathrm{cm}^2$-s, but return to nearly $10^{10}/\mathrm{cm}^2$-s on orbit 8278. *Strangeway et al.* [2000] show the outflow is correlated with the Poynting flux (bottom panels).

The extended period of strong ion outflow makes the September 25, 1998 cusp event a prime candidate for supplying ionospheric O^+ to the plasmasheet and eventually to the storm ring current. In addition, the high O^+ outflow energies reported by *Moore et al.* [1999] and observed by TIMAS were more than adequate for O^+ escape into the mantle and eventually into the plasmasheet. The peak of the magnetic storm occurred about 10 hours after the cusp ion outflows began which is adequate time for cusp plasma to convect across the pole and into the plasmasheet, and return to the nightside ring current.

What is not so clear is whether cusp ion outflows can account for the initial drop in Dst. A typical convection time for cusp field lines to move across the polar cap at hundreds of meters per second [*Dungey,* 1965] and return to the inner magnetosphere is ~4 hours. During active periods the cross polar cap potential can increase so the convection time may be reduced to as little as 2-3 hours. Dst had dropped to -85 at 2-3 UT and continued to -152 at 3-4 UT on September 25. Thus the initial phase of the magnetic storm could be due to cusp ion outflow being recycled to the inner magnetosphere. However, *Moore et al.* [1999] show that the cusp ion outflow was relatively high in velocity (~100 km/s) so that these ions would be far down the tail (>50 R_e) by the time the field line convected to the nightside oval. If a near Earth neutral line is providing reconnection in the tail, as expected during active periods, then much of the cusp outflow would be lost down the tail.

Another possibility is that a high density plasma was already present in the plasmasheet, or injected shortly after the arrival of the CME, and was subsequently convected into the inner magnetosphere causing the initial drop in Dst. FAST data show no atypical large cusp or large near-midnight outflows on orbits prior to the CME arrival. However, the northern border of the polar cap at 00:25 UT was located at ILAT~82° suggesting that a major substorm had occurred prior to the FAST pass. An examination of Polar UVI images shows that a major substorm began shortly after the arrival of the CME, with all of the nightside oval brightened, and with the near midnight brightening extending to ILAT> 80° (private communication, George Parks). AE rose from a little over 500 to nearly 2000 at the arrival of the CME indicating the CME probably triggered this intense substorm. As we will show below, intense outflows are observed from the nightside oval during substorms. Thus ion outflow associated with the substorm may have provided the initial plasma that formed the ring current during the early phase of this magnetic storm.

4. ION OUTFLOWS NEAR MIDNIGHT

Near midnight ion outflows fall into 3 categories: outflow associated with inverted-V electrons or upward current regions, outflow associated with upgoing electron beams or downward current regions, and outflow associated with counterstreaming electrons near the polar cap boundary. Plate 4 shows a FAST pass near midnight that contains all three outflows. Starting at the top, the panels show ion energy spectra, upgoing ion number flux between 20 and 1000 eV, electron spectra, electron pitch angles, and east-

ward magnetic perturbation field. A positive (negative) slope in the perturbation field denotes a downward (upward) east-west aligned current sheet. The period from 23:34:20 to 23:38:15 UT is an example of an upward current region where the low altitude ion outflows are typically low energy (<30 eV) conics that form more energetic ion beams as they pass through the inverted-V acceleration region. (An ion beam appears briefly in the top panel at 23:34:30 UT.) These conics are associated with electromagnetic ion cyclotron (EMIC) waves and typical fluxes are $< 10^8/\mathrm{cm}^2$-s when mapped to 100 km.

Ion outflow in the downward current region, 23:33:25-23:34:20 UT, consists of more energetic conics [*Carlson et al.,* 1998] trapped below a parallel electric field [*Gorney et al.,* 1985], with heating provided by broadband electric low frequency (BBELF) waves and/or electron solitary waves [*Ergun et al.,* 1998]. Although these ions constitute the highest energy conics, their fluxes are modest and similar to upward current region fluxes.

The region of ion outflow near the polar cap, 23:38:15 to 23:39:10, is associated with counterstreaming electrons and contains highly structured, filamentary, upward and downward currents (bottom panel). Velocity dispersed downgoing ions (although not clear in Plate 4) are often observed in this region showing that these outflows occur on newly reconnected field lines [*Zelenyi et al.,* 1990]. Polar cap boundary (PCB) ion conics constitute the most intense ion outflows observed during the FAST campaign, with typical fluxes of 10^8-$10^9/\mathrm{cm}^2$-s. The association of these outflows with BBELF and counterstreaming electrons suggests that these waves provide the ion heating and that the waves are generated by the counterstreaming electrons.

Using data from the FAST satellite, *Tung et al.* [2000] examined PCB ion conics and found a correlation of these outflows with substorms. Thus substorms represent a mechanism for injecting a large flux of ionospheric plasma into the plasmasheet. The observed outflows were primarily light ions, H^+ and He^+, rather than O^+. Total ion outflows above 20 eV were conservatively estimated (using a 1-2 hour local time extent) to be between 10^{23}/s and 10^{24}/s. These estimated outflows represent less than 1% of the average auroral outflows presented by *Yau et al.* [1985], and thus may seem unimportant to the total ion outflow budget. However, the DE-1 observations were taken near solar maximum and included non-winter hemisphere outflows, both of which can greatly enhance total outflow. The *Tung et al.* [2000] study took place in the winter hemisphere during solar minimum, and thus may not be representative of PCB conic outflow during more active or in sunlit conditions. Below we will show an example of a much larger PCB conic outflow associated with a magnetic storm where the conics are primarily O^+.

Plate 5 shows a PCB conic outflow event in the southern hemisphere during the magnetic storm on February 12, 2000, with the same format as Plate 4. This particular outflow occurred in the middle of the magnetic storm (Figure 1d) and during a period of enhanced AE (>1000). Plate 5 shows what may have been the beginning of a poleward expansion phase of a substorm since the aurora is rather far south (ILAT< 65°) but with fairly large energy flux (~ 10 ergs/cm^2-s). On the following orbit (~16 UT), the polar cap boundary was located at a more nominal ILAT~69° and the aurora was much weaker (<1 erg/cm^2-s). Counterstreaming electrons and the associated PCB ion conics were observed over 6° of invariant latitude. The PCB conic outflow in Plate 5 appears to encompass most of the width of the oval, with only diffuse aurora appearing to the south. Unlike the outflows described by *Tung et al.* [2000], this outflow was dominated by O^+. Low latitude ions observed by FAST were also primarily O^+. Since this outflow occurred in the summer hemisphere on the rise to solar max, enhanced solar output and sunlight conditions may explain the enhanced O^+.

Similar PCB conic outflows (10^9-$10^{10}/\mathrm{cm}^2$-s) were observed during the two previous FAST orbits. On orbit 13774, which skimmed along the auroral oval, PCB conic outflows were measured over a wide local time (1 to 8 MLT) demonstrating that during active periods these outflows are not necessarily restricted to midnight. The largest outflows ($> 10^{10}/\mathrm{cm}^2$-s) were also observed on this orbit (~10 UT) and may have provided the ionospheric plasma to the plasmasheet that subsequently formed the ring current, producing the peak in the magnetic storm (Figure 1d). Since this outflow was over a large local time range and with fluxes that were 1-2 orders of magnitude larger than those studied by *Tung et al.* [2000], it is likely that the PCB outflows dominated the total ion outflow.

As seen in Figure 1d, the provisional Dst for the February 12, 2000 magnetic storm begins in hour 9-10 UT with a drop from -25 to -94. The provisional Dst had a minimum of -169 in hour 11-12 UT, recovered to -124 in hour 13-14 UT, then remained near this value for about 5 additional hours before beginning a

rather rapid decay to greater than -60 the next day. If one tries to associate these drops in Dst with ion outflows observed on FAST and with enhanced AE, one can hypothesize the following.

We begin with the initial Dst drop at 3-4 UT on February 12. Three periods of enhanced AE were observed prior to the drop in Dst. No FAST auroral data were available for the first two periods, however FAST did measure near midnight outflows of $\sim 10^9/cm^2$-s at ~03:18 UT as AE declined to ~500. At this time the polar cap boundary was located at ILAT~74.5° near midnight and the PCB electron precipitation was weak (~1 erg/cm^2-s). These observations, when combined with a declining AE, indicate the 3:18 UT PCB outflow occurred at the end of a substorm expansion. If similar outflows occurred during the first two periods of enhanced AE, these ions would be convected into the inner magnetosphere during the third period of enhanced AE and may be responsible for the short drop in Dst in hour 3-4 UT on February 12.

We now examine the main phase of the magnetic storm. A fourth period of enhanced (>1000) AE occurred at 9:50-10:10 UT and is likely related to the strong southward B_z that began shortly before 8 UT. FAST observed extremely large PCB O^+ conic outflows ($\sim 10^{10}/cm^2$-s) at ~9:45 UT over an extended local time (1-8 MLT). This large outflow appears ~1 hour before the minimum Dst. The IMF had a strong southward component until ~11:30 UT and should have strongly driven magnetospheric convection. This suggests that the largest PCB conic outflow into the plasmasheet was likely convected to the inner magnetosphere and formed the ring current responsible for the minimum in Dst at 11-12 UT. AE continued to be relatively active and the following two FAST orbits measured additional intense PCB outflows (see Plate 5). These outflows provided additional ions to the plasmasheet which, when convected to the inner magnetosphere, may have kept Dst relatively low until ~19 UT. Although the above associations cannot prove that PCB outflows provide the ionospheric plasma that produced this magnetic storm, they provide strong circumstantial evidence that substorm outflows are a primary driver of Dst.

5. CONCLUSION

Models that attempt to predict the space weather associated with magnetic storms must be able to account for the relative abundance of ionospheric and solar wind plasma in the inner magnetosphere. Observations from FAST show that the low energy portion of the storm injected ring current is primarily of ionospheric origin and related to auroral activity as indicated by AE. Intense ion conic outflows from the cusp and a near midnight polar cap boundary (PCB) were examined for two storms. The cusp outflows were likely ejected out the tail whereas the substorm related PCB outflows contribute substantial ionospheric plasma to the plasmasheet. These observations suggest how substorms can play a role in the development of magnetic storms. Electrons accelerated near the polar cap boundary during substorms generate waves that heat the ionospheric plasma producing intense conic outflows into the plasmasheet. The higher density plasmasheet ions are subsequently convected to the inner magnetosphere by the large convection electric fields during the magnetic storm. Without the large convection fields associated with magnetic storms, the substorm outflows have no effect on Dst since these ions never reach the inner L-shells. Without substorm outflows, the plasmasheet density is relatively modest so that convection to the inner L-shells produces only small drops in Dst. In this model, it is through ionospheric ion outflows that substorms affect the development of magnetic storms.

Acknowledgments. The analysis of FAST data was supported by NASA grant NAG-3596. Dst values were obtained from the web site http://swdcdb.kugi.kyoto-u.ac.jp and we thank T. Kamei and M. Sugiura for preparation of these quantities.

References

Arnoldy, R. L., and K. W. Chan, Particle Substorms observed at the geostationary orbit, *J. Geophys. Res., 74,* 5019, 1969.

Carlson, C. W., et al., FAST observations in the downward auroral current region: energetic upgoing electron beams, parallel potential drops, and ion heating, *Geophys. Res. Lett., 25,* 2017, 1998.

Chen, M. W., L. R. Lyons, and M. Schulz, Simulations of phase space distributions of storm time proton ring current, *J. Geophys. Res., 99,* 5745, 1994.

Daglis, I. A., The role of magnetosphere-ionosphere coupling in magnetic storm dynamics, in Magnetic Storms, *Geophys. Mono. 98,* 107, 1997.

DeForest, S. E., and C. E. McIlwain, Plasma clouds in the magnetosphere, *J. Geophys. Res., 76,* 3587, 1971.

Dungey, J. W., The length of the magnetospheric tail, *J. Geophys. Res., 70,* 1753, 1965.

Ergun, R. E., et al., FAST satellite observations of large-amplitude solitary waves, *Geophys. Res. Lett., 25,* 2041, 1998.

Gorney, D. J., Y. T. Chiu, and D. R. Croley, Jr., Trapping of ion conics by downward parallel electric fields, *J. Geophys. Res., 90,* 4205, 1985.

Grafe, A., Are our ideas about Dst correct?, *Ann. Geophys., 17,* 1, 1999.

Greenspan, M. E., and D. C. Hamilton, A test of the Dessler-Parker-Sckopke relation during magnetic storms, *J. Geophys. Res., 105,* 5419, 2000.

Hamilton, D. C., et al., Ring current development during the great geomagnetic storm of February 1986, *J. Geophys. Res., 93*, 14,343, 1988.

Kamide, Y., et al., Magnetic storms: current understanding and outstanding questions, in "Magnetic Storms", *Geophys. Mono. 98,* 1, 1997.

Kozyra, J. U., et al., Effects of a high-density plasma sheet on ring current development during November 2-6, 1993, magnetic storm, *J. Geophys. Res., 103,* 26,285, 1998.

Lennartsson, W., R. D. Sharp, A comparison of the 0.1-17 keV/e ion composition in the near equatorial magnetosphere between quiet and disturbed conditions, *J. Geophys. Res., 87,* 6109, 1982.

Liemohn, M. W., et al., Analysis of early phase ring current recovery mechanisms during geomagnetic storms, *Geophys. Res. Lett., 26,* 2845, 1999.

Lockwood, M., et al., The cleft ion fountain, *J. Geophys. Res., 90,* 9736, 1985.

Mauk, B. H., and C. E. McIlwain, Correlation of Kp with the substorm-injected plasma boundary, *J. Geophys. Res., 79,* 3193, 1974.

McPherron, R. L., The role of substorms in the generation of magnetic storms, in "Magnetic Storms", *Geophys. Mono. 98,* 131, 1997.

Moore, T. E., et al., The cleft ion plasma environment at low solar activity, *Geophys. Res. Lett., 23,* 1877, 1996.

Moore, T. E., et al., Ionospheric mass ejection in response to a CME, *Geophys. Res. Lett., 26,* 2339, 1999.

Strangeway, R. J., et al., Cusp field-aligned currents and ion outflows, *J. Geophys. Res., 105,* 21129, 2000.

Tung, Y.-K., et al., Auroral polar cap boundary ion outflow observed on FAST, *J. Geophys. Res.,* in press, 2000.

Yau, A. W., et al., Energetic auroral and polar ion outflow at DE 1 altitudes: magnitude, composition, magnetic activity dependence, and long-term variations, *J. Geophys. Res., 90,* 8417, 1985.

Young, D. T., H. Balsiger, and J. Geiss, Correlations of magnetospheric ion composition with geomagnetic and solar activity, *J. Geophys. Res., 87,* 9077, 1982.

Zelenyi, L. M., R. A. Kovrazkhin, and J. M. Bosqued, Velocity-dispersed ion beams in the nightside auroral zone: AUREOL 3 observations, *J. Geophys. Res., 95,* 12119, 1990.

J. P. McFadden, Y. K. Tung, and C. W. Carlson, Space Sciences Laboratory, University of California, Berkeley, CA 94720. (e-mail: mcfadden@ssl.berkeley.edu)

E. Moebius and L. M. Kistler, Space Science Center, University of New Hampshire, Durham, NH 03824.

R. J. Strangeway, Institute of Geophysics and Planetary Physics, University of California, Los Angeles, CA 90095.

This preprint was prepared with AGU's LaTeX macros v5.01. File weather9˙website formatted October 13, 2000.

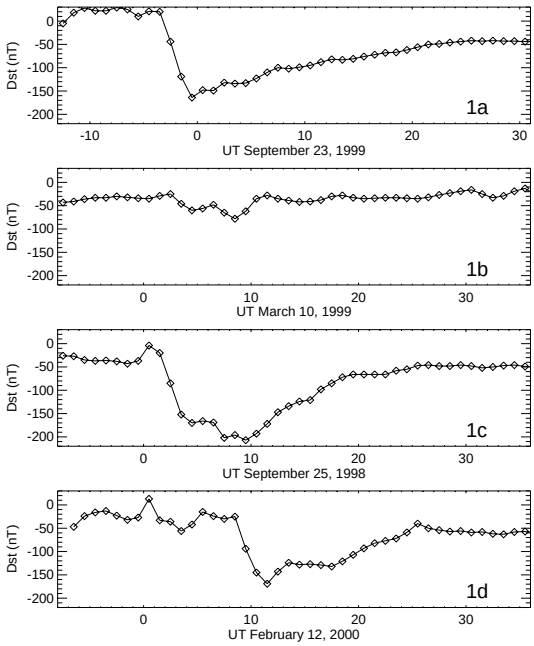

Figure 1. Dst for 99-9-23, 99-3-10, 98-9-25, and 00-2-12.

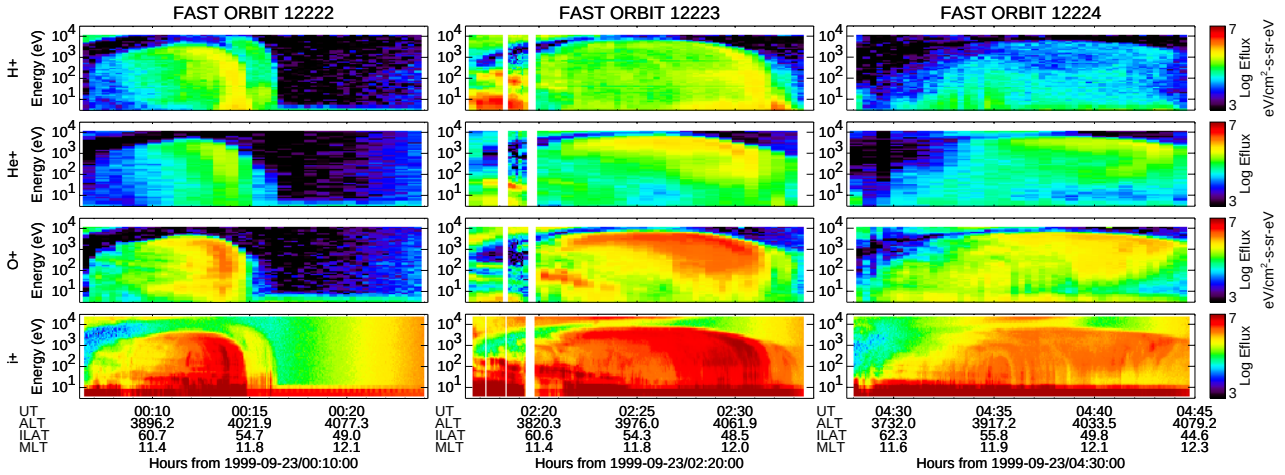

Plate 1. Plots of low latitude ion injections during FAST orbits 12222,12223,12224 on 99-9-23. This injection is characteristic of many injections observed by FAST during magnetic storms. The ion injection is primarily O^+ and evolves on two hour time scales. Penetrating radiation contaminates the ESA data (bottom plot) near 45° invariant latitude (ILAT).

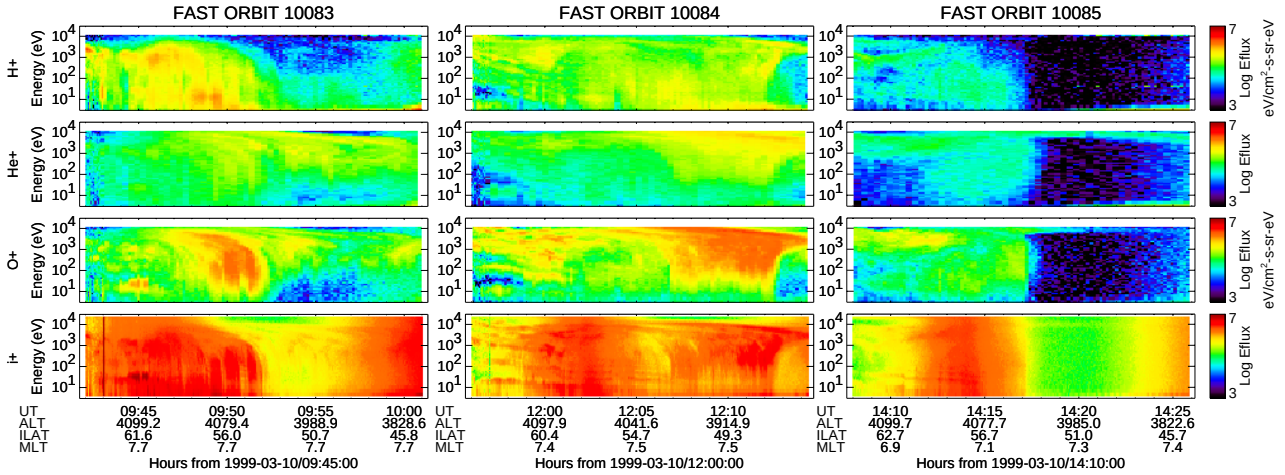

Plate 2. Plots of low latitude ion injections during FAST orbits 10083,10084,10085 on 99-3-10. Orbit 10083 has both a new injection ($> 54°$ ILAT) and the remains of an earlier injection ($< 54°$ ILAT). Orbit 10084 shows the evolution of the new injection from orbit 10083, and orbit 10085 shows the ions at ILAT$< 55°$ have disappeared due to co-rotation.

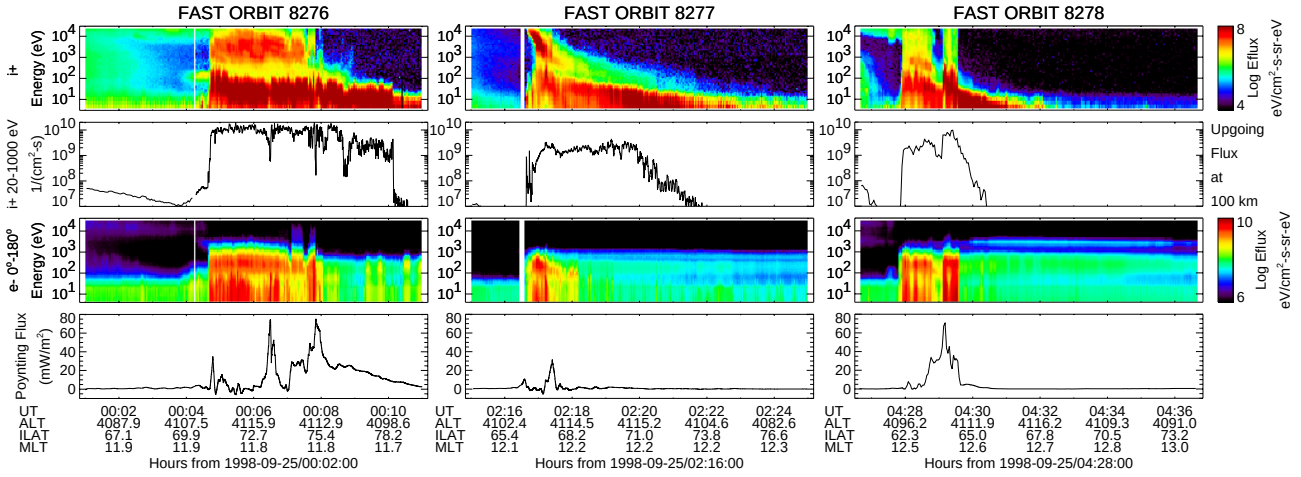

Plate 3. Ion spectrogram, upgoing ion flux, electron spectrogram and Poynting flux in the cusp for FAST orbits 8276, 8277, 8278 on 98-9-25. Conic outflows from the cusp during this magnetic storm were some of the largest observed during the FAST mission.

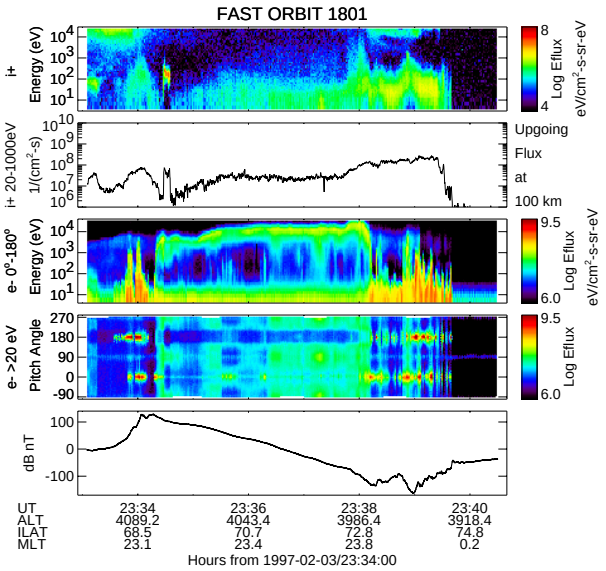

Plate 4. Ions, upgoing ion flux, electrons, electron pitch angle distribution, and magnetic field minus model field for a midnight crossing of the auroral oval. Plot shows conic outflows from the downward (~23:34 UT) and upward (23:34:20-23:38:10 UT) current regions are much smaller than polar cap boundary conic outflows (23:38:10-23:39:30).

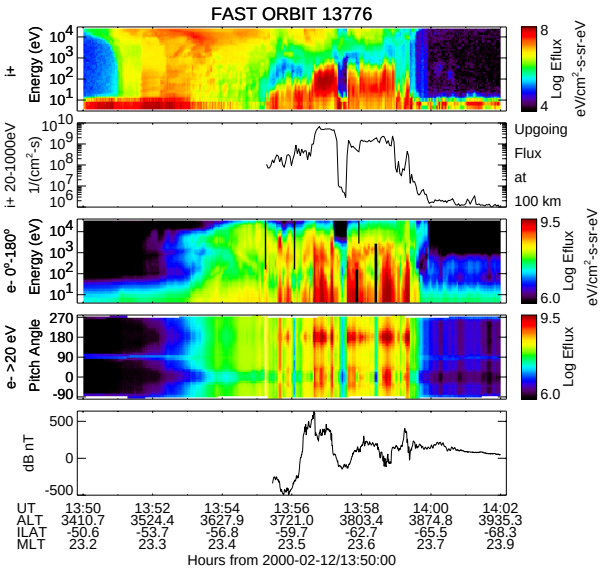

Plate 5. A polar cap boundary (PCB) conic outflow during the magnetic storm on 00-2-12. Format is the same as Plate 4. The figure shows PCB conic outflows (second panel) during magnetic storms can be as large as those observed from the cusp (Plate 3).